

# Synthesis of Ethyl Levulinate by a New Bio-Nanocatalyst

Maria Sarno<sup>ab</sup>, Mariagrazia Iuliano<sup>c,\*</sup>

<sup>a</sup>Department of Physics, University of Salerno, Via Giovanni Paolo II, 132 - 84084 Fisciano (SA), Italy

<sup>b</sup>Centre NANO\_MATES, University of Salerno Via Giovanni Paolo II, 132 - 84084 Fisciano (SA), Italy

<sup>c</sup>Department of Industrial Engineering, University of Salerno, via Giovanni Paolo II, 132 - 84084 Fisciano (SA), Italy  
[msarno@unisa.it](mailto:msarno@unisa.it)

Lipase from *Thermomyces lanuginosus* was physically anchored to AgAu-Fe<sub>3</sub>O<sub>4</sub>@tartaric acid nanoparticles (NPs) to be used for the conversion of levulinic acid into ethyl-levulinate, in the presence of ethanol. The proposed strategy explored the direct immobilization of the enzyme on the as-prepared tartaric acid modified NPs. A very remarkable conversion of 90 % was achieved at 4:1 ETOH/acid molar ratio, after 12 h and at 45°C reaction temperature, higher than that shown by free lipase.

## 1. Introduction

Lignocellulosic biomasses are accepted as a potential resource for the sustainable production of chemicals and fuels. Nowadays, a literature overview can give an immediate idea of the impressive amount of research currently performed around this topic, i.e., the fabrication of chemical platforms from biomasses.

Levulinic acid, formed from deep hydrolysis of lignocellulosic biomasses, belongs to this last class of compounds and results in a promising building block for chemistry. Levulinic acid derivatives such as alkyl-esters, which can be produced through homogeneous/heterogeneous catalysis, are chemicals of great interest. Ethyl-levulinate is an alkyl-ester of industrial significance, derived from levulinic acid through the esterification of carboxylic groups with fuel-grade ethanol. It has an oxygen content of 33% and properties similar to the biodiesel fatty acid methyl esters, which make it suitable to be used as an oxygenate diesel additive. Moreover, adding ethyl-levulinate into diesel engines results in a cleaner-burning fuel with flashpoint stability, high lubricity, improved viscosity and reduced sulfur content (Hayes, 2009). On the other hand, ethyl-levulinate can be also been applied in the flavoring and fragrance industries (Olson, 2001). The esterification reaction is usually carried out at high temperatures and in the presence of an acid catalyst such as sulphuric acids. The application of enzymes to the synthesis of esters has increased extensively in recent years. Enzymes catalyzed processes are an alternative to acid catalysts, indeed the enzymatic synthesis offers numerous advantages over conventional chemical esterification, such as (i) mild reaction conditions; (ii) minimal waste disposal; and, (iii) ease of product isolation. On the other hand, one main drawback of lipase-catalyzed processes is the high cost of the enzyme. The immobilization of enzymes onto nanomaterials is a topic of great interest. Indeed the reduction of the enzyme support size can provide a larger surface area for the attachment, leading to higher loading. The literature presents different nanomaterials for enzyme immobilization, such as (i) carbon nanotubes (CNTs); (ii) nanoparticles, magnetic nanoparticles (MNPs) (Sarno et al., 2017; Sarno and Iuliano 2018; Sarno and Iuliano 2019; Sarno and Iuliano 2020), (iii) nanocomposites, (iv) nanofibers, (v) nanorods and (vi) mesoporous media (Ahmad et al., 2015). Magnetic nanoparticles (MNPs) offer the added advantages of easy separation, lower leaching problems, and possible higher selectivity (Jia et al., 2003). Furthermore, Fe<sub>3</sub>O<sub>4</sub> magnetic nanoparticles have been regarded as promising supports because of biocompatibility and low cost (Hwang et al., 2013; Sarno et al., 2016; Sarno and Ponticorvo 2017). Immobilization can basically occur in different ways: by adsorption, covalent attachment, and encapsulation (Gupta et al., 2011).

This work aimed to synthesize ethyl-levulinate. Particular attention has been devoted to the optimization of the preparation of a new enzymatic catalyst, which consists of nanoparticles directly functionalized in a single step of synthesis to anchor the enzyme through physical bonds. Another important aspect is the choice of the surfactant, which can provide coordination with the nanoparticle, stabilizing them. Surfactants with -COOH

group, because of their strong affinity to  $\text{Fe}^{\text{III}}$  ions, were often chosen. In particular, here for the first time, L-(+)-tartaric acid (TA), with different carboxyl groups, has been selected to bond with the enzyme directly. Our experimental results evidence the one-step successfully immobilization of lipase on the as-produced nanoparticles. In particular, ethyl levulinate with high yield was obtained through esterification of levulinic acid and ethanol in the presence of *Thermomyces lanuginosus* lipase immobilized on an  $\text{AgAu-Fe}_3\text{O}_4@\text{tartaric acid}$  catalyst.

## 2. Materials & Methods

### 2.1 Synthesis Nanoparticles

All chemicals were acquired from Aldrich Chemical Co and are analytical grade.

The synthesis of nanoparticles was carried out at  $200^\circ\text{C}$  in an autoclave of capacity 50 ml for 6 h, a schematic representation of the synthesis apparatus was reported in Figure 1. Briefly, ferric chloride hexahydrate, silver nitrate ( $\text{AgNO}_3$ ) and gold(III) chloride trihydrate ( $\text{HAuCl}_4$ ) of 3 mmol, 0.1 mmol, and 0.1 mmol, respectively were added to L-(+)-tartaric acid (TA), 1 mmol, urea, 30 mmol, and 30 ml of ethylene glycol. The mixture was stirred for ~30 min at room temperature. Subsequently, the solution was placed in an autoclave. After 6 h the solution was cooled at room temperature and washed with 80 ml of ethanol, and water. Finally, the solid precipitate was dried at  $60^\circ\text{C}$  for 24 h, and the  $\text{AgAu-Fe}_3\text{O}_4@\text{TA}$  nanoparticles were obtained.

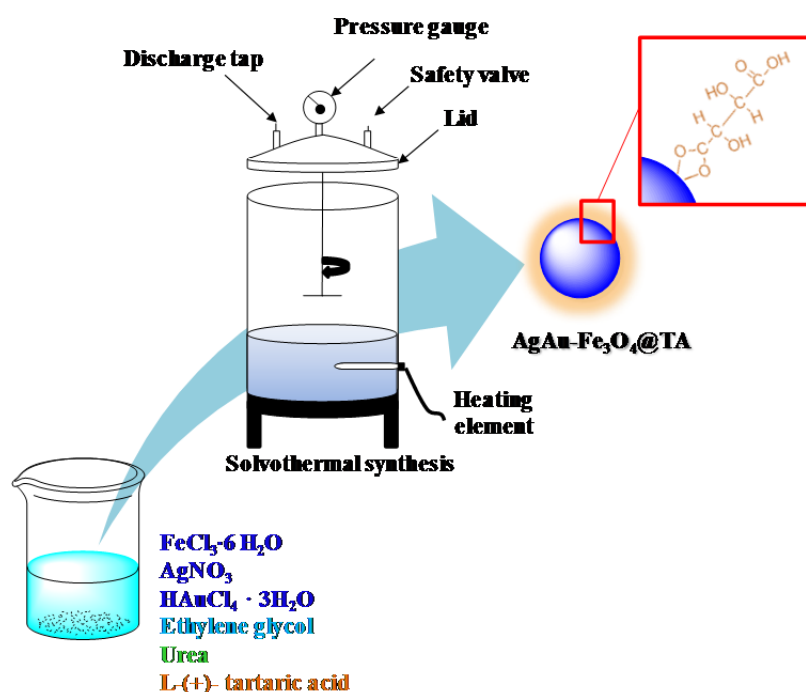


Figure 1: Preparation of  $\text{AgAu-Fe}_3\text{O}_4@\text{TA}$  nanoparticles

### 2.2 Enzyme immobilization and Hydrolytic activity

$\text{AgAu-Fe}_3\text{O}_4@\text{TA}$  can be used for direct immobilization of *Thermomyces lanuginosus* lipase (TL). In particular, the immobilized process was carried out into a glass flask containing 50 mg of nanoparticles and 10 mL of *Thermomyces lanuginosus* lipase (0.1 mg/mL, 1 M citrate buffer pH= 3). The glass flask was relocated into a temperature-controlled water bath shaker and shaken at  $4^\circ\text{C}$  for 3 h.

After 3 h, the immobilized enzyme was collected using a magnet and washed several times with 1 M citrate buffer to remove free enzyme. The immobilization efficiency (%) was determined by a UV-visible spectrophotometer (Evolution 60S, Thermo Scientific) at a wavelength of 595 nm by the Bradford method (Bradford, 1997). Moreover, hydrolytic activity of the immobilized and free lipase were measured by using titrimetric assays based on an olive oil emulsion method (Abrami et al., 1999; Sarno et al., 2019). In particular, the quantity of the hydrolyzed fatty acids was determined by the titration of the fatty acids derived from the hydrolysis of olive oil with a standard KOH solution (0.1 M). One unit of enzymatic activity for the immobilized

lipase was defined as the amount of enzyme that released 1  $\mu\text{mol}$  of fatty acids per minute under the assay conditions. The activity recovery (%) was evaluated as the ratio between the lipase activity of the immobilized lipase and the activity of the free lipase.

### 2.3 Esterification of Levulinic acid into Ethyl Levulinate catalyzed by immobilized lipase

Commercially available levulinic acid is used as a model compound in order to produce levulinate esters. Levulinic acid was reacted with ethanol see Figure 2, at EtOH/Acid molar ratio of 1:1 M, 2:1 M, 4:1 M, and 6:1 M) for 12 h, 45  $^{\circ}\text{C}$  and under stirring in the presence of immobilized lipase (catalyst concentration: 5 wt% of LA). Ester yields were measured by detecting the amount of free LA through titration with 0.02 M NaOH in the presence of phenolphthalein.

The product was analyzed in a Thermo-Fischer gas chromatography equipment, capillary column (Trace-GOLD TG-POLAR GC Columns 0.25  $\mu\text{m}$  $\times$ 0.25 mm $\times$ 60 m). Helium was used as carrier gas with a flow rate of 1.2 ml/min. The starting temperature of the column was 40 $^{\circ}\text{C}$  and it was gradually raised at the rate of 20  $^{\circ}\text{C}/\text{min}$  to a temperature of 275  $^{\circ}\text{C}$  for 5 min, while the injector and detector were maintained at 250  $^{\circ}\text{C}$ .

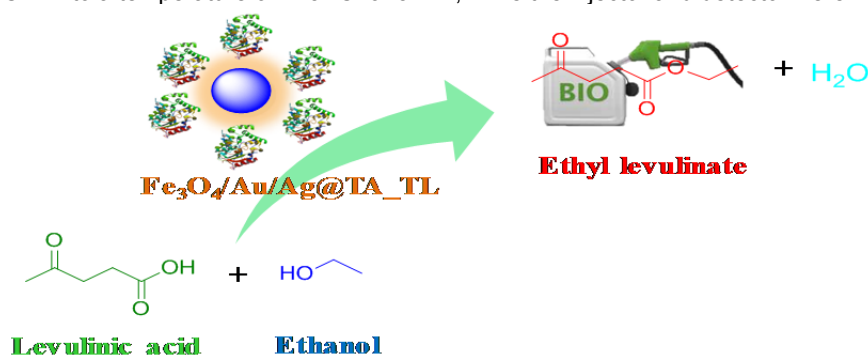


Figure 2: Esterification of levulinic acid to ethyl levulinate through  $\text{AgAu-Fe}_3\text{O}_4@TA\_TL$  nano-bio catalyst.

## 3. Results & Discussion

### 3.1 Catalysts Characterization Results

The TEM images show the tartaric acid-coated  $\text{AgAu-Fe}_3\text{O}_4$  nanoparticles, see Figure 3a. In particular, the  $\text{AgAu-Fe}_3\text{O}_4$  NPs displayed a spherical morphology with an average diameter of 9 nm, while the nanoparticles of Au and Ag showed an average size lower than 3 nm.

Figure 3b shows an X-ray (XRD) diffraction spectrum of  $\text{AgAu-Fe}_3\text{O}_4@TA$  nanoparticles. It is possible to see the typical peaks of magnetite at 30.1 $^{\circ}$  (220), 35.6 $^{\circ}$  (311), 43.1 $^{\circ}$  (400), 53.4 $^{\circ}$  (422), 57.2 $^{\circ}$  (511) and 62.5 $^{\circ}$  (440) (Sarno et al., 2017). Furthermore, there are also the typical silver peaks, at 46.1 $^{\circ}$ , 64.2 $^{\circ}$  and 76.8 $^{\circ}$  (Zhang et al., 2012) and gold peaks, at 38.31 $^{\circ}$  (111), 44.46 $^{\circ}$  (200), 64.67 $^{\circ}$  (220) and 74.45 $^{\circ}$  (331) (Zhang et al., 2012; Sarno et al., 2018).

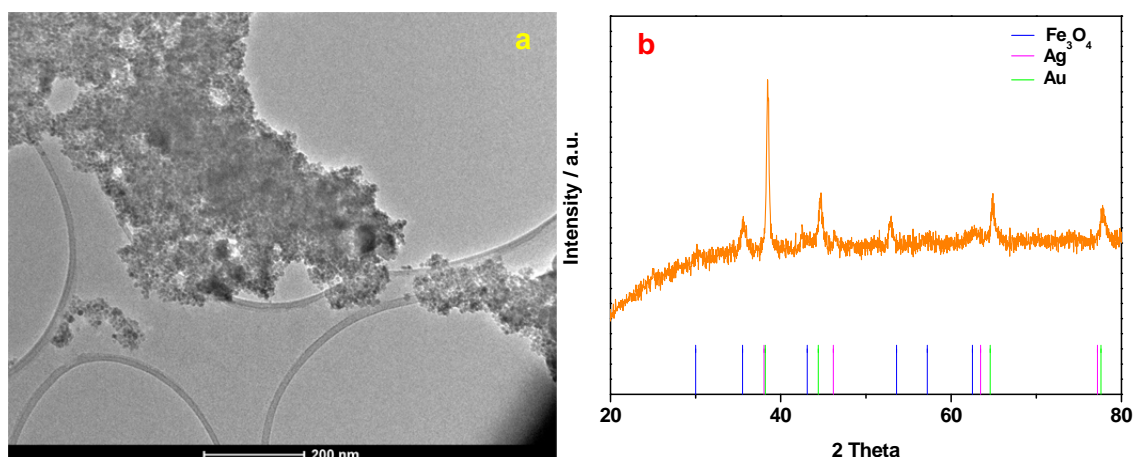


Figure 3: TEM image of  $\text{AgAu-Fe}_3\text{O}_4@TA$  nanoparticles

### 3.2 FT-IR analysis

The FT-IR spectra in Figure 4 show the profiles of Tartaric acid (TA), AgAu-Fe<sub>3</sub>O<sub>4</sub>@TA, AgAu-Fe<sub>3</sub>O<sub>4</sub>@TA-TL, and free TL. The TA profile shows a dominant peak at 1740 cm<sup>-1</sup>, resulting from the carbonyl stretch C=O associated with protonated carboxyl groups (Moovendaran et al., 2014) which was reduced in intensity with adsorption/chemisorption of TA on AgAu-Fe<sub>3</sub>O<sub>4</sub> as the carboxyl groups deprotonated in AgAu-Fe<sub>3</sub>O<sub>4</sub>@TA nanoparticles. As the intensity of the carbonyl peak waned at AgAu-Fe<sub>3</sub>O<sub>4</sub>@TA, peaks at 1644 cm<sup>-1</sup> and 1393 cm<sup>-1</sup> appeared. These two features represent the asymmetric and symmetric stretching of COO<sup>-</sup> groups anchored on the nanoparticles (Jia et al., 2012), respectively (Li et al., 2013).

AgAu-Fe<sub>3</sub>O<sub>4</sub>@TA-TL FT-IR spectrum after immobilization evidence the presence of a number of functional groups of the lipase structure, indeed after immobilization, the FT-IR spectrum frequencies of the main bands for lipase can be observed (Sarno et al., 2019). Peaks at 1659 cm<sup>-1</sup> and 1550 cm<sup>-1</sup> are due to N-H bending vibrations typical of lipase and correspond to amide I and amide II bands (Atacan et al., 2015; Atacan et al., 2016), their shift suggesting protein conformation change and hydrogen bond interaction between the enzyme and support (Atacan et al., 2015; Atacan et al., 2016; Sarno et al., 2019). These results suggest the physical adsorption of the TL on the magnetic nanoparticles.

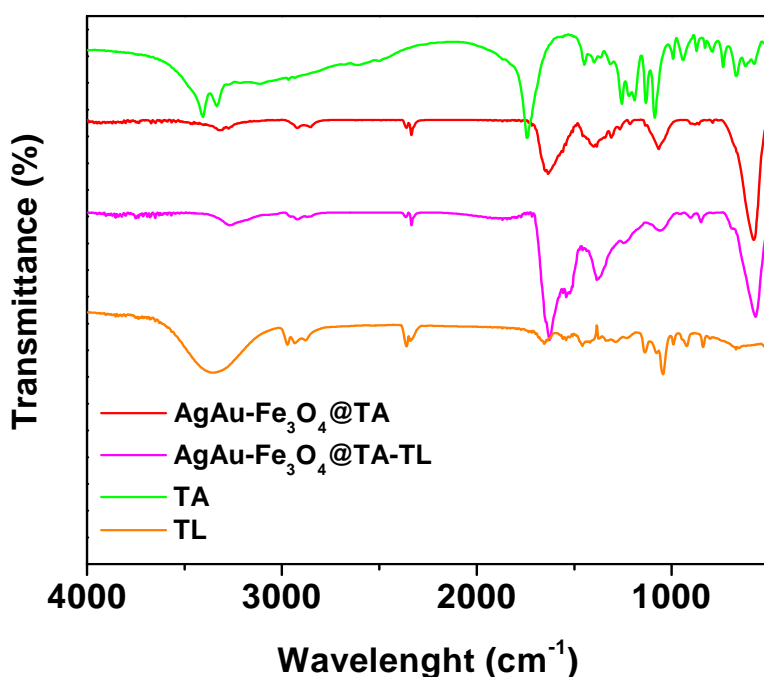


Figure 4: FT-IR spectra in the range of wavenumber 4000-500 cm<sup>-1</sup> of nanoparticles synthesized (AgAu-Fe<sub>3</sub>O<sub>4</sub>@TA), nanoparticles after lipase immobilization (AgAu-Fe<sub>3</sub>O<sub>4</sub>@TA-TL), L-(+)-tartaric acid (Sigma Aldrich, TA) and *Thermomices lanuginous* lipase (Sigma Aldrich, TL).

### 3.3 Effect of time on immobilization efficiency and activity recovery

The results of the experiments performed with immobilized enzymes shown in Figure 5 highlights the efficiency of the immobilization as a function of coupling time. The immobilization efficiency on the AgAu-Fe<sub>3</sub>O<sub>4</sub>@TA support increase quickly when the time increase from 60 min to 120 min, due to the free carboxyl groups still present on the support, while the immobilization efficiency slows after 120 min probably due to saturated binding sites on the support, which eventually prevent further enzyme acceptance. Diffusion restrictions observed in these situations exert further strain on enzyme catalysis, difficult substrate entrance to the active site and product release (Bayramođlu et al., 2010). Under coupling times increase the activity recovery of the immobilized enzyme increase. This can be attributed to the conformational flexibility of the enzyme on the support (Ma et al., 2009).

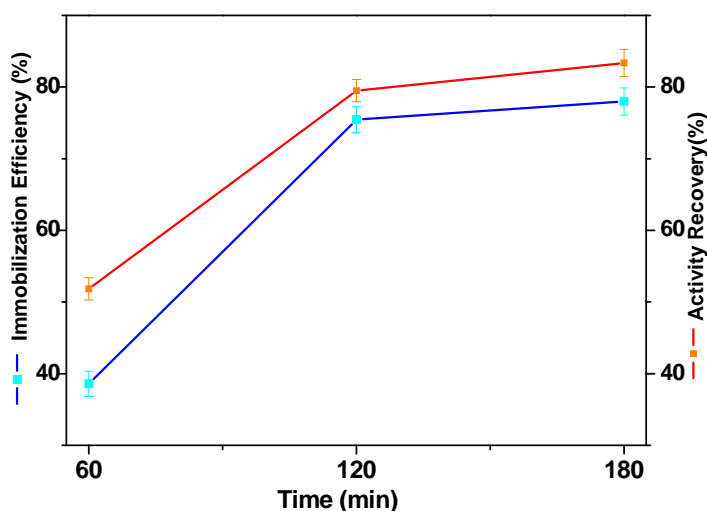


Figure 5: Effect of the time on the lipase loading, immobilization efficiency, and activity recovery. Immobilization condition: coupling temperature, 4°C; coupling pH, 3; lipase amount, 1 mg/ml.

### 3.4 Effect of molar ratio on the esterification process

The mole ratio of ethanol to levulinic acid was varied from 1:1 to 6:1 at a catalyst loading of 5% (g enzyme/g levulinic acid) at 45°C for 12 h (see Figure 6). The ester yield (%) increase for the immobilized enzyme from 53 % to ~90 % when the ethanol to levulinic acid molar ratio increase from 1:1 to 4:1 M. On the other hand, for free lipase, the ester yield increases much slowly and only up to about ~72 % at the molar ratio of 4:1, probably due to the water formation that slow the kinetic reaction. At molar ratio ethanol to levulinic acid of 4:1 for immobilized lipase and free lipase, the yield decreases probably due to ethanol inducing catalyst deactivation (Bi et al., 2016), and may reflect the fact that alcohol can deviate the essential water layer from the enzyme (Syamsu et al., 2010).

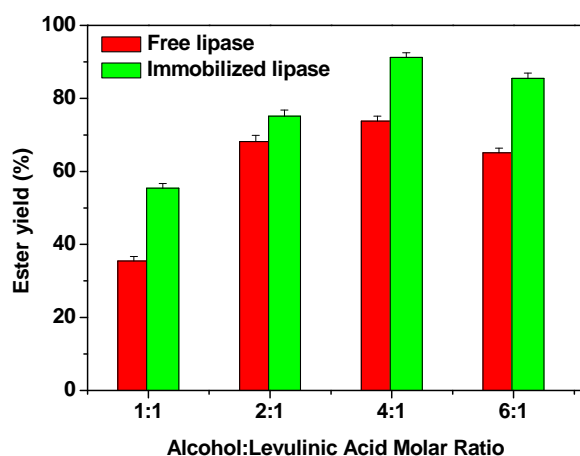


Figure 6: Effect of alcohol to oil molar ration on free and immobilized lipase for ester synthesis. Immobilization condition: coupling temperature, 4°C; coupling time, 3 h; coupling pH, 3; lipase amount, 0.1 mg/ml. Reaction conditions: reaction time, 12 h; reaction temperature, 45°C; lipase concentration, 5%.

## 4. Conclusions

In summary: nanoparticles coated with tartaric acid were successfully synthesized. High immobilization efficiencies, about 78 %, was obtained at pH 3 on the optimized tartaric acid modified nanoparticles. The immobilized lipase shows an activity recovery up to 80 % after 180 min of immobilization time. Immobilized *Thermomyces lanuginosus* lipase is able to catalyze the synthesis of ethyl levulinate in a solvent-free system, successfully. The substrate molar ratio is the significant process variable that affected the synthesis of

the levulinate ester. A high percentage conversion (~90.0%) is achieved in a 12 h for immobilized lipase. The above results indicate that immobilized TL is a promising platform for the immobilization of lipase to catalyze the synthesis of alkyl levulinates.

## References

- Abrami M, Lešćić I., Korica T., Vitale L., Saenger W., Pigac J., 1999, Purification and properties of extracellular lipase from *Streptomyces rimosus*, *Enzyme and Microbial Technology*, 25, 522–529.
- Ahmad R., Sardar M., 2015, Enzyme Immobilization: An Overview on Nanoparticles as Immobilization Matrix, *Biochemistry and Analytical Biochemistry*, 4, 1000178.
- Atacan K., Çakıroğlu B., Özacar M., 2016, Improvement of the stability and activity of immobilized trypsin on modified Fe<sub>3</sub>O<sub>4</sub> magnetic nanoparticles for hydrolysis of bovine serum albumin and its application in the bovine milk, *Food Chemistry*, 212 460–468.
- Atacan K., Özacar M., 2015 Characterization and immobilization of trypsin on tannic acid modified Fe<sub>3</sub>O<sub>4</sub> nanoparticles, *Colloids and Surfaces B: Biointerfaces*, 128, 227–236.
- Bayramoğlu G., Metin A.U., Altintas B., Arica M.Y., 2010, Reversible immobilization of glucose oxidase on polyaniline grafted polyacrylonitrile conductive composite membrane. *Bioresource Technology*, 101, 6881–6887.
- Bi Y., Yu M., Zhou H., Zhou H., Wei P., 2016, Biosynthesis of oleyl oleate in solvent-free system by *Candida rugosa* Lipase (CRL) immobilized in macroporous resin with cross-linking of aldehyde-dextran, *Journal of Molecular Catalysis B: Enzymatic*, 133, 1-5.
- Gupta M.N., Kaloti M., Kapoor M., Solanki K., 2011, Nanomaterials as Matrices for Enzyme Immobilization, *Artificial Cells Blood Substitutes and Biotechnology*, 39, 98-109.
- Hayes D.J., 2009, An examination of biorefining processes, catalysts and challenges, *Catalyst Today*, 145, 138-151.
- Hwang E.T., Gu M.B., 2013, Enzyme stabilization by nano/microsized hybrid materials, *Engineering in Life Sciences*, 13, 49–61.
- Jia H., Zhu G., Wang P., 2003, Catalytic behaviors of enzymes attached to nanoparticles: the effect of particle mobility, *Biotechnology and Bioengineering*, 84, 406–414.
- Jia J., Yu J. C., Zhu X.-M., Chan K. M., Wang Y.-X. J., 2012, Ultra-fast method to synthesize mesoporous magnetite nanoclusters as highly sensitive magnetic resonance probe, *Journal Colloid Interface Science*, 379, 1-7.
- Li W., Zhang B., Li X., Zhang H., Zhang Q., 2013, Preparation and characterization of novel immobilized Fe<sub>3</sub>O<sub>4</sub>@SiO<sub>2</sub>@mSiO<sub>2</sub>-Pd(0) catalyst with large pore-size mesoporous for Suzuki coupling reaction, *Applied Catalyst A*, 459, 65.
- Ma S., Mu J., Qu Y., Jiang L., 2009, Effect of refluxed silver nanoparticles on inhibition and enhancement of enzymatic activity of glucose oxidase, *Colloids and Surfaces A: Physicochemical and Engineering Aspects* 345, 101-105.
- Moovendaran K., Jayaramkrishnan V., Natarajan S., 2014, Optical Studies on L-Tartaric acid and L-Proline Tartrate, *Photonics and Optoelectronics*, 3, 9.
- Olson E.S., 2001, Conversion of Lignocellulosic Material to Chemicals and Fuels, Energy & Environmental Research Center. University of North Dakota
- Sarno M., Iuliano M., 2018, Active biocatalyst for biodiesel production from spent coffee ground, *Bioresource Technology*, 266, 431-438.
- Sarno M., Iuliano M., 2019, G-Fe<sub>3</sub>O<sub>4</sub>/Ag supporting *Candida rugosa* lipase for the “green” synthesis of pomegranate seed oil derived liquid wax esters, *Applied Surface Science*, 510, 145481.
- Sarno M., Iuliano M., 2019, Highly active and stable Fe<sub>3</sub>O<sub>4</sub>/Au nanoparticles supporting lipase catalyst for biodiesel production from waste tomato, *Applied Surface Science*, 474, 135-146.
- Sarno M., Iuliano M., Polichetti M., Ciambelli P., 2017, High activity and selectivity immobilized lipase on Fe<sub>3</sub>O<sub>4</sub> nanoparticles for banana flavor synthesis, *Process Biochemistry*, 56, 98-108.
- Sarno M., Ponticorvo E., 2017, Much enhanced electrocatalysis of Pt/PtO<sub>2</sub> and low platinum loading Pt/PtO<sub>2</sub>-Fe<sub>3</sub>O<sub>4</sub> dumbbell nanoparticles, *International Journal of Hydrogen Energy*, 42, 23631-23638.
- Sarno M., Cirillo, C., Scudieri, C., Polichetti M., Ciambelli P., 2016, Electrochemical Applications of Magnetic Core-Shell Graphene-Coated FeCo Nanoparticles, *Industrial and Engineering Chemistry Research*, 55, 3157-3166
- Syamsu K.M.W., Salina M.R., Siti S.O., Hanina M.N., Basyaruddin M.A.R., Jusoff K., 2010, Green Synthesis of Lauryl Palmitate via Lipase-Catalyzed Reaction, *World Applied Science Journal*, 11, 401-407.
- Zhang Y., Gao G., Qian Q., Cui D., 2012, Chloroplasts-mediated biosynthesis of nanoscale, Au-Ag alloy for 2-butanone assay based on electrochemical sensor, *Nanoscale Research Letters*, 7, 475.